A New Numerical Method for Potential Analysis and Design of Hybrid Components from Full Vehicle Simulations: Implementation and Component Design

Thomas Tröster[1](✉), Alan A. Camberg[1], Nils Wingenbach[1],
Christian Hielscher[2], and Julian Grenz[2]

[1] Automotive Lightweight Design, Paderborn University, Mersinweg 7,
33100 Paderborn, Germany
{thomas.troester,alan.camberg,
nils.wingenbach}@uni-paderborn.de
[2] BENTELER Automobiltechnik GmbH, 1 An der Talle 27–3,
33102 Paderborn, Germany
{christian.hielscher,julian.grenz}@benteler.com

Abstract. To exploit the lightweight potential of common materials like steel, aluminum or especially fiber-reinforcement plastics (FRP), a load-compliant material concept is mandatory. In keeping with the motto "the best material for the best application", a new approach for a tailored material distribution between FRP and metals is proposed. By defining a scalar value referred as "uniaxiality" and a uniaxiality weighted sensitivity, a numerical method is implemented to identify body-in-white (BIW) components with a high amount of anisotropic loading. The uniaxiality value is gathered from full vehicle crash simulations and is superpositioned over all load cases to access a generalized information which component's area is suitable for isotropic materials like metals and which one for anisotropic materials like FRP. In the next step, a functional component group consisting of an A-pillar and a roof frame section is exemplary engineered by using the findings of the numerical potential analysis. The developed extreme lightweight concept made of aluminum extrusion, unidirectional carbon fiber-reinforcement plastics (CFRP) tapes, warm stamped aluminum and press-hardened steel demonstrates outstanding performance that has been proven in full vehicle crash simulations and experimental tests. Furthermore, the concept is evaluated in terms of the components CO_2 footprint and costs. Based on these data a scalable component concept is possible to meet customer specific requirements between the design objectives: lightweight, costs and environmental impact.

Keywords: Potential analysis · Hybrid components · Finite element analysis · Crash simulation · Multi-material design

1 Introduction

Hybrid material concepts, as an approach to combine the advantages of two different materials by compensating their disadvantages at the same time, have attracted increased interest in both academia and industry [1]. In recent years, several hybrid components concepts have been introduced into automotive series production. The front roof frame of the Audi A6 (C6, model year 2004) is one of the first examples of how weight reduction can be realized by combining different materials while maintaining cost neutrality [2]. Another early example of hybrid lightweight design is the sidewall frame of a small-series hydrogen derivate of the BMW 7-series (E68, model year 2005). To fulfil the strict safety requirements of a hydrogen-powered vehicle, the steel sidewall frame was reinforced by CFRP patches [3]. The hybrid reinforcement concept allowed a cost-effective solution for small series with high flexibility and quick integration into the existing production process. In addition, a weight saving of 52% compared to a steel solution was achieved [4]. With the new BMW 7 Series (G11, model year 2015), several hybrid components consisting of steel shell structures and CFRP reinforcement patches have been introduced into series production, enabling mass savings of up to 40 kg per BIW [5, 6]. A hybrid lightweight design approach is also featured in the body structure of the new BMW 8 Series (G15, model year 2018) [7]. The latest convertible model of the iconic sports car Porsche 911 (992, model year 2019) uses hybrid parts as well [8]. Here, the hybrid A-pillar is manufactured using a technology developed within the Q-Pro project [9]. Based on the examples given, it can be concluded that hybrid lightweight design is an interesting and promising lightweighting strategy not only from a research point of view, but also from that of industry.

However, the design of lightweight and efficient multi-material concepts requires a detailed information about the stress and strain distributions within a component. This applies in particular to the use of FRP, since the mechanical properties of fiber-based materials are highly dependent on the loading direction. This fact is crucial for applications with different load cases, such as a car body structure that must provide high stiffness under operational loads and a high level of passive safety in any crash scenario. These challenging requirements lead often to conservative designs that do not exploit the full lightweight potential of the materials used. Such as in the hybrid B-pillar of the BMW 7 Series (G11), where the CFRP patch has a quasi-isotropic layup [6].

To increase the utilization rate of FRP in complex car body structures, Durst [10] proposed a method that identifies the suitability of FRP for car body components by evaluating the stress state over different load cases. The method is based on the product of three factors: the principal stress ratio, the variation in the load direction and a load case-weighting factor given by the sum of the absolute values of the major and minor principal stress. The result is a scalar value per every BIW component that characterizes the averaged anisotropy state of the component. Albers et al. [11] presented an enrichment of the method from [10] into the 3D stress space. Furthermore, not only the averaged component's anisotropy value but also the local (element) specific anisotropy value can be evaluated by a contour plot. Klein et al. [12] presented

a further enhancement of the method from [10] by introducing a new approach for the load case superposition and by considering several possible fiber orientations. Moreover, the anisotropy value is additionally weighted by stiffness and strength factors. A significant enrichment of Durst's method was proposed by Dlugosch [13]. The introduction of a so-called *principal stress factor* enables a stress tensor addition over several load cases through a modification of the initial stress tensors. An undeniable advantage of this method is the implicit consideration of loading directions and absolute stress values. A further criterion introduced by Dlugosch is the *uniformity* as a component specific degree of homogeneity in the loading directions. Later, both component-specific values are combined to an *anisotropy coefficient* which gives the components suitability for FRP reinforcements. Moreover, the vector of the resulting loading orientation can be plotted element-wise directly on the component's geometry enabling the deduction of an optimized ply design directly from the results of the anisotropy analysis. Eventually, Grote [14] proposed a further improvement to the method from [10]. By introducing a "force flow" weighted orientation factor, material thickness is considered and high loads have a greater impact on the resulting orientation of the superpositioned anisotropy value. Unlike in [10, 11, 12], Dlugosch [13] and Grote [14] applied their methods not only to stiffness but also to crash problems.

With the aim to design components with a highly effective and targeted use of FRP materials, a new design methodology for hybrid components is proposed within this paper. A uniaxiality analysis in analogy to [13] is implemented to analyze the accumulated principal stresses. However, instead of using a generalized *uniformity* value to characterize the FRP-suitability of the whole component, the uniaxiality values are used to weight local sensitivities and identify component areas with a high potential for local FRP reinforcements. The methodology is applied on a full vehicle model in several crash load cases. In a further step, a chosen component group with a high fraction of uniaxial loading is redesigned by taking into account local sensitivities and loading anisotropies. Finally, the a newly designed hybrid car body component is manufactured and tested on a dynamic crash device.

2   Proposed Approach

To pursue an affordable and demand-oriented lightweight design of hybrid BIW components, a stress-based potential analysis in analogy to the *principal stress factor* from [13] is implemented and enhanced by a uniaxiality weighted sensitivity analysis. Starting with benchmark simulations of a full vehicle model, a cumulative anisotropy analysis of each component is performed and a crash-relevant body assembly with a high overall uniaxiality is selected for a hybrid design trial. The single components are optimized with the proposed method and adapted for multi-material design. The core idea of the method is to use unidirectional fiber materials in areas with high anisotropic loads and to carry the isotropic part of the load through a metallic part. In addition, the CO_2 footprint and costs are also evaluated during the design phase of the component. In the final design step, the crashworthiness of the newly designed hybrid assembly is determined in full vehicle simulations and compared with the benchmark

structure. The objective is to reduce the weight of the components while maintaining or even increasing the crash performance of the vehicle. The design procedure conducted in this work is shown in Fig. 1.
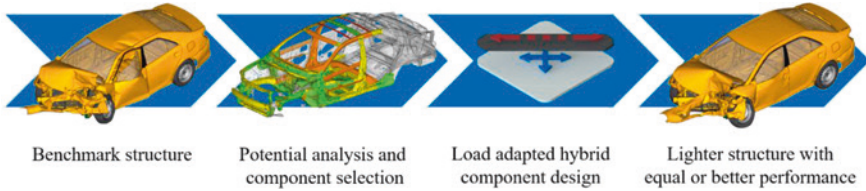

Benchmark structure   Potential analysis and   Load adapted hybrid   Lighter structure with
                       component selection   component design   equal or better performance

Fig. 1. Proposed approach for analyzing and improving mechanical structures by lightweight hybrid components.

2.1 Uniaxiality Analysis

In analogy to Dlugosch's *principal stress factor* [13], the here presented approach is based on the definition of a scalar value that characterizes the so-called *uniaxiality U* of the stress tensor. As given in Eq. (1), the uniaxiality describes the magnitude of the ratio between the absolute value of the second and first principal normal stress. This characteristic value takes amounts between 0 and 1, where $U = 1$ describes a purely uniaxial (anisotropic) and $U = 0$ a purely equi-biaxial (isotropic) stress state, see Fig. 2. As in [13], the load case superposition is based on the addition of stress components. A specific modification of stresses ensures that the summation does not lead to the annulment of values with different signs. At the same time, it is ensured that the original load direction and the absolute stress values are maintained. The advantage of this procedure is that information about the direction of the resulting stresses remain available and that the individual time steps and load cases are weighted by the magnitude of the stress values. The resulting uniaxiality is determined in the last step from the accumulated stress tensor. The detailed sequence of the algorithm is given in Fig. 3.

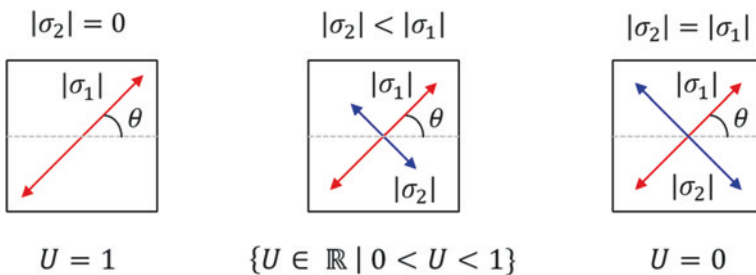$$U = 1 - \frac{|\sigma_2|}{|\sigma_1|}, \quad |\sigma_1| \geq |\sigma_2| \quad (1)$$

$|\sigma_2| = 0$ $|\sigma_2| < |\sigma_1|$ $|\sigma_2| = |\sigma_1|$

$U = 1$ $\{U \in \mathbb{R} \,|\, 0 < U < 1\}$ $U = 0$

Fig. 2. Uniaxiality values of chosen stress states.

In the here used approach, first the element's stress tensor $\tilde{\sigma}^e$ is evaluated at the most loaded integration point (IP) of a reduced-integrated element type (element type 2 from the LS-DYNA standard element library) with five through-thickness IP and stored for each individual timestep i of the load case j (1). Subsequently, the angle θ_{ij}^e of the principal axis system in relation to the element coordinate system is determined (2) and the absolute values of the principal normal stresses are computed (3). By assuming that tensile and compressive stresses are equivalent, it is ensured that stresses of different signs do not lead to a cancellation of the values during summation. In the next step, a modified element stress tensor $\tilde{\sigma}_{ij}^{e*}$ is computed from the absolute values of the principal normal stresses with the original angle θ_{ij}^e of the principal normal stresses (4). In the next step, all $\tilde{\sigma}_{ij}^{e*}$ values are accumulated to a resulting stress tensor $\tilde{\sigma}^{e**}$ (5). The tensorial value guarantees a weighting of the individual timestep and load case entities during summation and provides information about the resulting orientation of the superimposed stress tensors $\tilde{\sigma}_{ij}^{e*}$. The scalar value of the element uniaxiality U^e is determined in the very last step from the absolute values of the principal normal stresses of the accumulated stress tensor $\tilde{\sigma}^{e**}$ (6).
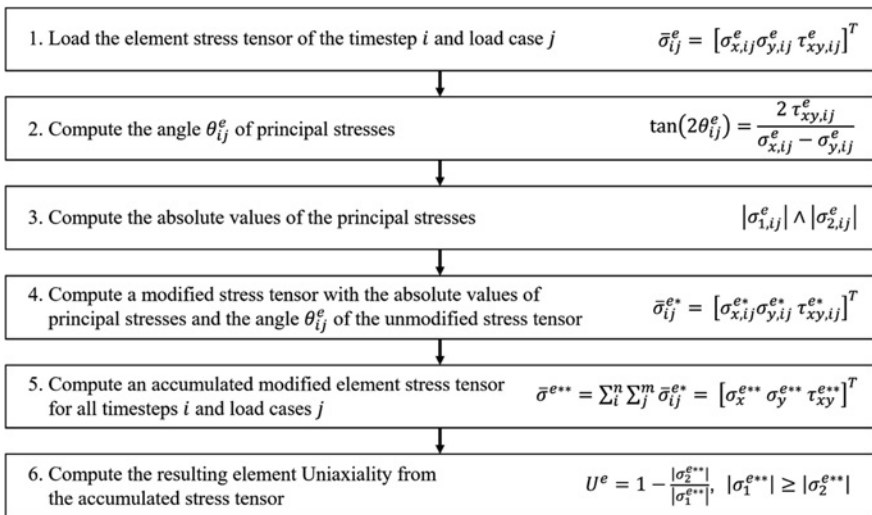

1. Load the element stress tensor of the timestep i and load case j	$\bar{\sigma}_{ij}^e = \left[\sigma_{x,ij}^e \sigma_{y,ij}^e \tau_{xy,ij}^e \right]^T$
2. Compute the angle θ_{ij}^e of principal stresses	$\tan(2\theta_{ij}^e) = \dfrac{2\, \tau_{xy,ij}^e}{\sigma_{x,ij}^e - \sigma_{y,ij}^e}$
3. Compute the absolute values of the principal stresses	$\left\| \sigma_{1,ij}^e \right\| \wedge \left\| \sigma_{2,ij}^e \right\|$
4. Compute a modified stress tensor with the absolute values of principal stresses and the angle θ_{ij}^e of the unmodified stress tensor	$\bar{\sigma}_{ij}^{e*} = \left[\sigma_{x,ij}^{e*} \sigma_{y,ij}^{e*} \tau_{xy,ij}^{e*} \right]^T$
5. Compute an accumulated modified element stress tensor for all timesteps i and load cases j	$\bar{\sigma}^{e**} = \sum_i^n \sum_j^m \bar{\sigma}_{ij}^{e*} = \left[\sigma_x^{e**} \sigma_y^{e**} \tau_{xy}^{e**} \right]^T$
6. Compute the resulting element Uniaxiality from the accumulated stress tensor	$U^e = 1 - \dfrac{\|\sigma_2^{e**}\|}{\|\sigma_1^{e**}\|}, \ \|\sigma_1^{e**}\| \geq \|\sigma_2^{e**}\|$

Fig. 3. Scheme of the implemented algorithm for an accumulated Uniaxiality analysis.

In the next step a component specific uniaxiality U^K value is calculated by averaging the element values over the component domains K. With the component specific uniaxiality value U^K, a fast identification of body parts (components) with a high overall uniaxiality fraction is possible. That enables an efficient determination of parts with a high potential for hybrid lightweight design.

2.2   Uniaxiality-Weighted Sensitivity Analysis

Once the uniaxiality analysis has been completed and a car body component with a high total anisotropic loading has been selected for hybrid redesign, a so-called *uniaxiality-weighted sensitivity analysis* of the component is carried out. In order to ensure that the expensive reinforcement fibers are used in areas with pronounced uniaxiality and at same time have a large effect on the structural performance of the component, a procedure depicted in Fig. 4 is introduced.

First, the baseline component K_b is divided into p reasonable subdomains $K_{b,c}$ that gauge sizes T_c are parametrized within a design space given by manufacturing and package restrictions. In the next step, a structural sensitivity analysis of the relevant system response with respect to each design variable is carried out. In parallel, a uniaxiality analysis of each component subdomain of the baseline design is computed. By multiplying the subdomain sensitivity with the subdomain uniaxiality value, a uniaxiality-weighted sensitivity is obtained. Finally, the weighted sensitivities are sorted in descending order to give an indication of which cross-sectional area of the component can be effectively reinforced by fibers in terms of structural performance and costs. With these data and a linear mixing rule of the material fractions within the respective subdomains, a minimization of the component mass M_b and the production greenhouse gas (GHG) emissions E_b can be performed. The production GHG emissions are calculated by multiplying the resulting material fractions φ_c by the material specific emission intensities I. The linear mixing rule is applied in such a way that a structural equivalence to the baseline design is given in terms of stiffness and strength.
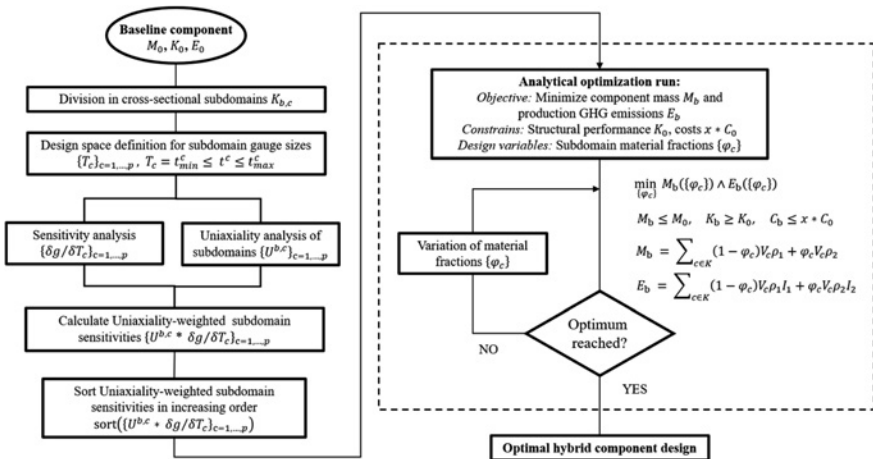

Fig. 4. Flowchart of the uniaxiality-weighted sensitivity analysis and the subsequent optimization loop for the design of sustainable lightweight hybrid components.

3 Accumulated Uniaxiality Analysis

The full vehicle model of the Toyota Camry 2012 [15] provided by the Center for Collision Safety and Analysis, George Mason University, is used as a benchmark structure. The relevant load cases are chosen under the consideration of the crash scenario probability in real traffic events. As reported in [16], frontal impact crashes dominate the total number of impacts (65.7%), followed by side impacts (27.3%). Consequently, worst-case configurations of European and US rating agency front and side crash load cases are selected for benchmarking, i.e. the Euro NCAP Moderate Overlap Deformable Barrier Frontal Test (64 km/h), the US NCAP Full-Width Rigid Wall Frontal Test (56 km/h), the IIHS Small Overlap Rigid Barrier Frontal Test (64 km/h), the US NCAP Side Moving Deformable Barrier Test (62 km/h) and US NCAP Side Pole Test (32 km/h). In order to consider all load case scenarios acting on the front and side area of the passenger compartment, the IIHS Roof Crush Test is incorporated into the benchmarking as well.

The uniaxiality analysis algorithm presented in Sect. 2.1 is implemented as a Tcl/Tk script into the Altair HyperView post-processor software. In order to ensure that the evaluation only takes place on structure-relevant components, a set of body-in-white components is created before the evaluation routine is started. A further measure to reduce the amount of data evaluated is realized by defining a threshold value for critical stress values (e.g. $\sigma_{yield}/2$). As soon as the FE solver output data of all load cases are available, all relevant elements run through the routine depicted in Fig. 3. The result is a contour plot as shown in Fig. 5, in which the uniaxiality can be displayed in the post-processor either as averaged component values or by element. In addition, the resulting direction of the accumulated element stresses can be displayed directly on the elements (not depicted here). With this information, the resulting fiber direction can be determined at the same time without additional computational effort.

Remarkably, several components in Fig. 5 show a uniaxiality value greater than 0.7, what means that the major principal stress is more than 3 times higher than the minor principal stress. As expected, bending dominated components, such as door beams, roof cross members or A-pillars, have a higher uniaxiality value than structures with multiple local buckling modes, such as front longitudinal members or crash boxes. When evaluating the element-wise uniaxiality, numerous areas of almost pure uniaxial loading can be identified.
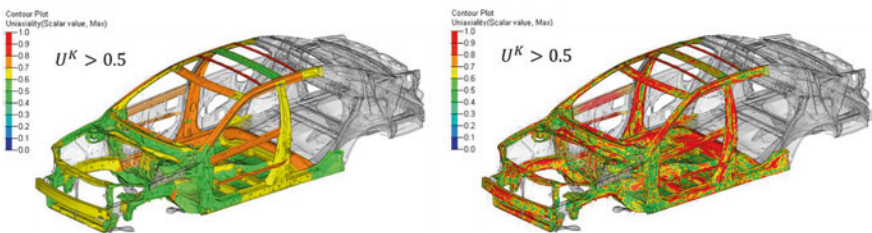

Fig. 5. Result of the uniaxiality analysis over several crash load cases for selected BIW components, threshold: $U^K > 0.5$; Left: Averaged component uniaxiality U^K, Right: Element uniaxiality U^e.

4   Component Design

4.1   Component Selection

The uniaxiality analysis serves as a starting point for the redesign of a selected component with a high hybridization potential. From that, the A-pillar and the front roof frame were selected as a demonstrator group. These components show a high uniaxiality and represent a part of the rigid passenger compartment. Both are excellent prerequisites for the efficient use of local reinforcements made of orthotropic and high-strength carbon fiber composites. In addition, the A-pillar offers not only the potential for increasing passive safety but also the possibility of extending the field of vision, which represents a secondary effect of higher weight-specific properties of this component. Furthermore, the A-pillar gained a lot of attention as a possible hybrid component in the past. Already in 2002, Liedke [17] examined the substitutability of a hybrid lightweight design approach for an A-pillar of a convertible derivate. Using two press-hardened steel shells and a load-adapted aramid-carbon fiber laminate reinforcement, a mass reduction of 12.4% was achieved while maintaining the same crash behavior. Today, the current BMW 7 Series [6] and the current Porsche 911 convertible (-2.7 kg / per vehicle) [8] use hybrid A-pillars in series production. Hence, it is particularly interesting to what design concept and results in weight reduction the development method presented here will lead to.

4.2   Component Design

At the beginning of the component development, a topology study was carried out. Based on the ideal component topology, several structural concept designs were derived, which were evaluated and compared using simplified finite element models. The most promising concept—a continuous and extruded aluminum profile with unidirectional reinforcement tapes—was refined in detail in further development stages. The design method presented in Sect. 2.2 was decisive for the location and the cross-section design of the reinforcing carbon fiber tapes. Unfortunately, the cross-sectional areas with the highest potential fall in the area of joining flanges and are therefore not suitable for fiber reinforcement, as this would lead to a complicated and costly joining situation. However, the selected positions of the carbon fiber unidirectional (UD) reinforcement tapes are located as close as possible to the joining flanges and correspond to a complementary upper and lower belt of the AA6082 T6 aluminum profile.

The lower A-pillar base was designed as a press-hardened steel shell due to a predominant multi-axial loading. The joining between the aluminum and steel parts of the A-pillar could be realized by conventional spot welding thanks to BENTELER-patented SWOPtec joining elements. The Flash Forming Process (FFP) [18], another technology patented by BENTELER, made it possible to manufacture the front roof frame from an AA5182 aluminum sheet and achieve strengths of up to 400 MPa.

Despite a high degree of uniaxiality, the front roof frame could not be designed as a hybrid with any significant mass advantage. The reason for this was the structural instability caused by local fiber reinforcements and the associated abrupt changes in stiffness. The connector node between the A-pillar profile and the roof frame is made of an AA6082 T6 aluminum extrusion, whose cross-section was designed by topology optimization. The final assembly design and the hybrid A-pillar cross-section is depicted in Fig. 6.
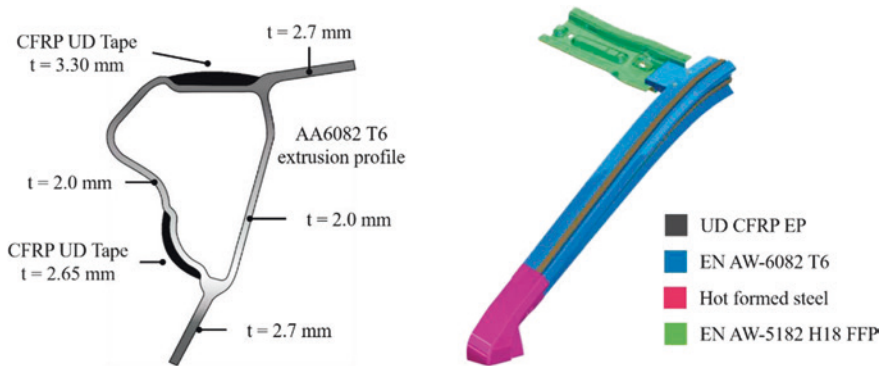
Fig. 6. Left: Hybrid A-pillar cross-section, Right: Final multi-material assembly design.

4.3 CO_2 Footprint and Cost Analysis

Lightweight design not only needs to deliver parts with lower mass, but also ensure moderate costs and a lower CO_2 footprint over the product life cycle. For this reason, a simplified eco-audit and a cost analysis of the hybrid A-pillar were carried out. The cost analysis assumed a production of 60,000 vehicles per year, which corresponds to a usual number of units in the premium segment, for which the use of CFRP is realistic. Even though CFRP was used very targeted, it was not possible to achieve cost neutrality compared to performance equivalent variants in aluminum (+14% weight) and press-hardened steel (+46% weight). The aluminum variant offers a cost-saving potential of 36% and the press-hardened steel variant is even 54% more cost-effective than the hybrid lightweight variant. When evaluating the CO_2 footprint, which was done using the CES Selector software, the hybrid A-pillar shows the lowest end-of-life CO_2 footprint of all concepts. Remarkably, the hybrid concept has a lower CO_2 footprint than the aluminum variant already from the beginning of the use phase, see Fig. 7.
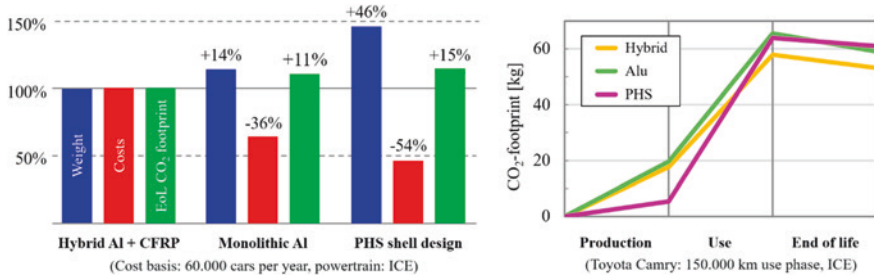
Fig. 7. Cost and simplified Life Cycle Assessment analysis of the hybrid A-pillar and performance equivalent aluminum and steel variants.

4.4   Full Vehicle Validation

Finally, the hybrid A-pillar design concept is validated in full vehicle crash simulations. An equivalent or better structural performance was achieved compared to the benchmark. In particular, the frontal load cases show an increase in passive safety, since the hybrid A-pillar, unlike the baseline design, does not buckle and provides a rigid passenger compartment. A comparison for the Euro NCAP Moderate Overlap Deformable Barrier Frontal Test (64 km/h) between the baseline and the hybrid design is presented in Fig. 8. The hybrid A-pillar provides structural integrity, reduced intrusions and lower maximum decelerations (-12.5%).
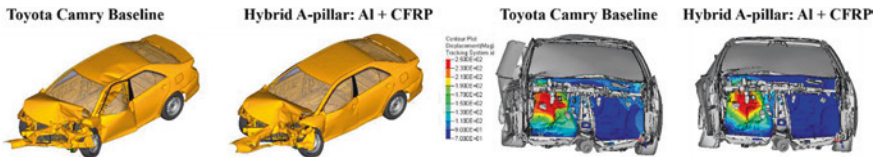

Fig. 8. Euro NCAP MODB Frontal Test (64 km/h): Baseline vs. Hybrid design. Left: Firewall intrusion in mm.

5   Component Manufacturing and Testing

The developed hybrid A-pillar cross-section profile was extruded from AA6082 and stretch-bended by BENTELER Aluminum Systems Norway AS, Raufoss. The unidirectional CFRP tapes (SGL SIGRAPREG® C U300-0/NF E420/38%) were manufactured using a tailored tape placement process at the Institute for Lightweight Design with Hybrid Systems (ILH), Paderborn. The simultaneous curing and bonding of the tapes to the extruded aluminum profile were realized by means of a prepreg press technology using an additional adhesive layer (3M SAT 1010). For comparison purposes, an unreinforced aluminum profile and an aluminum profile with an alternative

reinforcement made of a 1.8 mm DP800 steel were manufactured as well. The DP800 reinforcement strips where bonded to the aluminum profile by steel blind rivets (GESIPA G-Bulb 6,4 mm) and a structural adhesive (Dow Automotive BETAMATE 2096).

The crashworthiness of the developed A-pillar cross section (see Fig. 6) was investigated using a representative profile length of 400 mm in a three-point bending test on a drop tower device of the LiA Crash & Impact Lab. The support distance was set to 275 mm, the support and impactor radii were 25 mm. The impact energy was 2.0 kJ at an initial impact speed of 4.5 m/s. The results of the impact tests are summarized in Table 1. The force-displacement curves and post-crash pictures of the deformed profiles are given in Fig. 9. It is shown that the performance of the CFRP and steel reinforced profiles is comparable. Both profiles show a similar increase in maximum force and absorbed energy. However, the achieved mass specific energy absorption (SEA) shows a strong dependence on the reinforcement material. While the SEA increases by 32% for the CFRP reinforcement, it decreases by 5% for steel reinforcement compared to the unreinforced aluminum profile. The test results emphasize the performance of the hybrid aluminum CFRP profile.

Table 1. Experimental results of the energy absorption characteristics of the developed hybrid A-pillar.

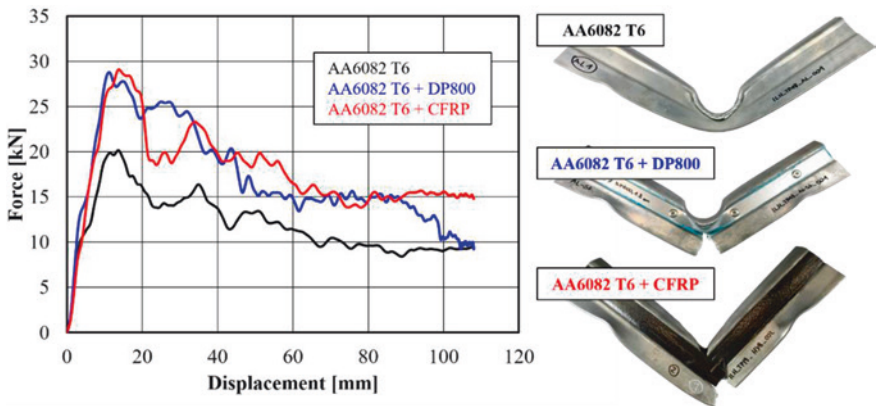| Specimen	Weight [kg]	F_{max} [kN]	E_{abs} [kJ]	SEA [kJ/kg]
AA6082 T6	0.556	20.16	1.29	2.32
AA6082 T6+CFRP	0.627 (+12.8%)	29.10 (+44%)	1.92 (+49%)	3.07 (+32%)
AA6082 T6+DP800	0.847 (+52.3%)	28.78 (+43%)	1.87 (+44%)	2.20 (−5%)

Fig. 9. Force-displacement curves and post-crash pictures of different A-pillar profiles.

6   Conclusions

Based on the findings of the accumulated uniaxiality analysis and the uniaxiality-weighted sensitivity, the design of components with targeted use of unidirectional fiber reinforcement in combination with classical isotropic metallic materials is possible. As shown by the example of the A-pillar, by substituting a material fraction of just two cross-sectional areas by a structural-equivalent amount of unidirectional carbon fibers, the components weight can be reduced by 14%. By means of a simplified life cycle assessment, it was possible to show that the hybrid component has even a better CO_2 footprint already in the production phase than a monolithic aluminum variant. Nevertheless, it was found that the cost of the hybrid component significantly exceeds that of conventional design concepts. This is mainly due to high material and additional processing costs. It must therefore be considered on individual use-case basis whether lower weight and environmental impact is justified by additional costs. However, with smaller production volumes the cost advantages of conventional concepts are reduced, so that a hybrid component concept can be economically reasonable if the requirements for lightweight are particularly high and the number of units is small. That could be particularly the case for derivate-dependent adjustment in crash performance due to e.g. a heavier powertrain. Furthermore, if the results are transferred to electric vehicles, the growing share of renewable energy sources will increase the importance of the production phase in terms of CO_2 emissions in the future, so that the development of sustainable material and component concepts will become increasingly important.

Finally, the hybrid A-pillar developed using the proposed numerical design method was able to prove its outstanding performance in full vehicle crash simulations and experimental impact tests. This confirmed the importance of smart product design methods and shows that the lightweight potential of hybrid components is far from being fully exploited.

References

1. Bader, B., Türck, E., Vietor, T.: Multi material design. A current overview of the used potential in automotive industries. In: Dröder, K., Vietor, T. (eds.) Technologies for Economical and Functional Lightweight Design, pp. 3–13. Springer, Berlin (2019)
2. Jäschke, A., Dajek, U.: Dachrahmen in Hybridbauweise. Sonderdruck aus VDI-Tagungsband Nr. **4260**, 25–45 (2004)
3. Müller, C., Fürst, S., von Klitzing, W.: Hydrogen safety: new challenges based on BMW hydrogen 7. In: Proceedings of 2nd International Conference on Hydrogen Safety 2007, San Sebastian (2007)

4. Derks, M.: CFK-Technologien im Automobilbau. DLR Wissenschaftstag 2007, Braunschweig. BMW Group, München (2007)

5. N.N.: Technical Training – Product Information – G12 Introduction. BMW AG (2015)

6. Frei, P.: The hybrid B-Pillar in the new BMW 7-Series. An Example for the manufacturing implementation of an innovative Steel-CRFP lightweight design concept. In: Automotive Circle, Materials in Car Body Engineering Conference, Bad Nauheim (2016)

7. Henseler, U., Eras, A.: Introducing the new 8 series coupe. In: Euro Car Body Conference, Bad Nauheim (2018)

8. Wawers, U., Stein, S.: The development and production of the new Porsche 911 body structure: the new 911 Carrera. In: Eckstein, L. (ed.) Proceedings of Aachener Body Engineering Days 2019. Institut für Kraftfahrzeuge, RWTH Aachen, Aachen (2019)

9. Haider, D.R., Krahl, M., Koshukow, W., Wolf, M., Liebsch, A., Kupfer, R., Gude, M.: Adhesion studies of thermoplastic fibre-plastic composite hybrid components part 2: thermoplastic-Metal-Composites. In: Hausmann, J.M., Siebert, M., von Hehl, A. (eds.) Proceedings of 3rd Hybrid Materials and Structures 2018, pp. 68–73. DGM, Berlin (2018)

10. Durst, K.G.: Beitrag zur systematischen Bewertung der Eignung anisotroper Faserverbundwerkstoffe im Fahrzeugbau. Cuvillier, Stuttgart (2008)

11. Albers, A., Schmid, A., Zhang, Q., Grönheim, O., Schipperges, J.: Ein CAE-basiertes Konzept zur automatischen Identifikation von Leichtbauteilen im Gesamtsystem. NAFEMS Magazin **23**(3/2012), 54–63 (2012)

12. Klein, D., Witzgall, C., Wartzack, S.: Bewertung und Optimierung der Faserverbundeignung von Leichtbaustrukturen in den frühen Phasen der Produktentwicklung. NAFEMS Magazin **32**(4/2014), 55–66 (2014)

13. Dlugosch, M.: Zur Methodenentwicklung im Entwurf automobiler Strukturkonzepte in FVK-Metall Hybridbauweise unter Crashbelastung. Schriftenreihe Forschungsergebnisse aus der Kurzzeitdynamik, Bd. 36. Fraunhofer Verlag (2018)

14. Grote, M.: Entwicklung einer Methode zur anforderungsgerechten Werkstoffauswahl und Strukturauslegung von PKW-Karosserien im Multi-Material-Design. Siegener Schriftenreihe Automobiltechnik, Bd. 2. Universitätsverlag Siegen, Siegen (2018)

15. Marzougui, D., Brown, D., Park, H.K., Kan, C.D., Opiela, K.S.: Development & validation of a finite element model for a mid-sized passenger Sedan. In: Proceedings of the 13th International LS-DYNA Users Conference, Dearborn, MI (2014)

16. Kramer, F.: Integrale Sicherheit von Kraftfahrzeugen, 4th edn. Springer, Wiesbaden (2013)

17. Liedtke, B.: Faserverbundkunststoff/Metall-Hybridstrukturen im Pkw-Rohkarosseriebau. Fortschritt-Berichte VDI: Reihe 12, Verkehrstechnik, Fahrzeugtechnik 509. VDI-Verlag, Düsseldorf (2002)

18. Camberg, A.A., Bohner, F., Tölle, J., Schneidt, A., Meiners, S., Tröster, T.: Formability enhancement of EN AW-5182 H18 aluminum alloy sheet metal parts in a flash forming process: testing, calibration and evaluation of fracture models. IOP Mat. Sci. Eng. **418**, 012018 (2018)